Photocatalytic degradation of hydrocarbons and methylene blue using floatable titanium dioxide catalysts in contaminated water

T. Schnabel, N. Jautzus, S. Mehling, C. Springer and J. Londong

ABSTRACT

Photocatalytic disintegration is a novel approach to eliminate pollution. The method utilizes the semiconductor titanium dioxide to degrade organic molecules in the presence of ultraviolet (UV) light. In this study, it is shown how the capabilities of several types of catalyst designs degrade the non-polar substance diesel fuel and the polar substance methylene blue. The floating design of foam glass coated with titanium dioxide could reduce the concentration of diesel fuel by 329 mg/L in 16 h; the submerged designs for coated glass fiber and coated steel grit could reduce methylene blue concentration by 96.6% after 4 h and 99.1% after 6 h, respectively. It could be shown that photocatalysis is a promising cost- and energy-efficient method for managing air and water pollution. It can be established as a low-technology method without requiring the use of a conventional source of energy, given an adequate amount of sun hours, or as an additional cleaning stage in water treatment plants using UV-LEDs.

Key words | clean-up, mineral oil, petrol-derived hydrocarbons, photocatalysis, titanium dioxide

T. Schnabel (corresponding author)
Department for Construction and Environmental Chemistry,
Laboratory for Material Testing and Research (MFPA) Weimar,
Weimar,
Germany
E-mail: *tobias.schnabel@mfpa.de*

N. Jautzus
S. Mehling
J. Londong
Chair for Urban Water Management and Sanitation,
Bauhaus-Universität Weimar,
Weimar,
Germany

C. Springer
Chair for Urban Water Management and Environmental Technology,
Erfurt University of Applied Sciences,
Erfurt,
Germany

HIGHLIGHTS

- Floating photocatalysts for solar photocatalysis.
- Low tech application for the treatment of surface water.
- Inexpensive material based on titanium dioxide.

doi: 10.2166/wrd.2021.118

GRAPHICAL ABSTRACT

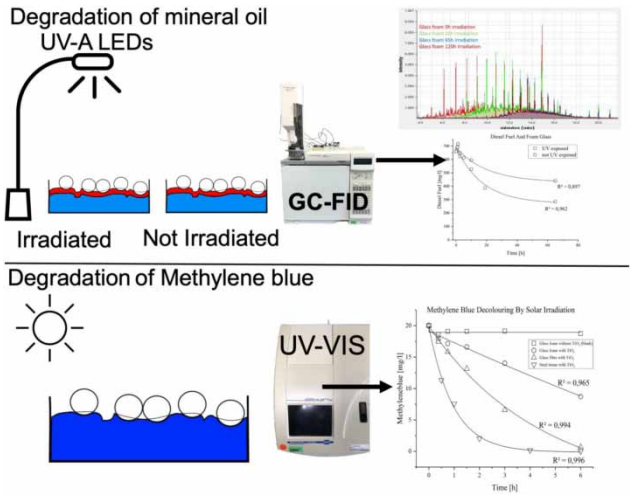

INTRODUCTION

Mineral oil-based pollution of water bodies is a problem worldwide today. The sources of pollution are diverse and include roadways, accidents, pollution from shipping, etc. Polluted water can be found in rainwater retention areas, docks, and, ultimately, in the natural water resources. Additionally, anthropogenic trace substances, such as pharmaceuticals, additives from personal care products, industrial chemicals, and pesticides, have been the focus of urban water management research for some time (Bergmann *et al.* 2011). Particularly in the context of further wastewater treatment, these substances and the process-technical possibilities for their elimination from water are considered.

Separation and/or degradation of contaminants from water is possible through physical, chemical, and biological means. While biological approaches rely on natural self-purification capabilities of the water body, this may take a considerable amount of time and results may be unsatisfactory (Weichgrebe *et al.* 1991). Physical and chemical methods tend to be more cost-intensive but offer faster results than biological methods (Pinnekamp *et al.* 2010). Precipitation, flocculation, disinfection, radiation, reverse osmosis, electro-coagulation, and absorption by activated charcoal are conventional methods (Pinnekamp *et al.* 2010).

Flexible and decentralized solutions are especially required in the case of accidents involving the release of large quantities of mineral oil hydrocarbons. Furthermore, increasing demand and parallel scarcity of freshwater and increasing pollution of water bodies, especially in developing countries and areas with insufficient infrastructure, create the need for a sustainable low-cost alternative for water clean-up. Particularly in warm regions, which receive high solar radiation throughout the year, a possible answer could be the use of solar-powered photocatalytic purification.

The novel approach of solar photocatalysis presented here relies on ultraviolet (UV) radiation from the sun that triggers the semiconductor characteristics of titanium dioxide (Pitre *et al.* 2017). The activation of the semiconductor is shown in Equation (1) (Nosaka & Nosaka 2013):

$$TiO_2 + h_v \rightarrow e^-_{cb} + h^+_{vb} \quad (1)$$

$$h^+_{vb} + R \rightarrow R^{\bullet +} \quad (2)$$

$$h^+_{vb} + H_2O \rightarrow OH^\bullet + H^+ \quad (3)$$

$$h^+_{vb} + OH^- \rightarrow OH^\bullet \quad (4)$$

$$e^-_{cb} + O_2 \rightarrow O_2^{\bullet -} \quad (5)$$

When irradiated by sunlight, titanium dioxide forms highly reactive oxygen species that can disintegrate organic molecules to their mineral components (Pedanekar *et al.* 2020) and are potentially lethal to microbes and can even destroy viruses (Cabiscol 2000). Several important features for the heterogeneous photocatalysis have extended its feasible applications in water treatment, such as ambient operating temperature and pressure, complete mineralization of organic substances, their derivate and decomposition products without secondary pollution, as well as low operating costs (Chong *et al.* 2010). It is well-documented (Mehrjouei *et al.* 2015) that highly reactive oxygen species cause cell lysis, generated as a result of the photo-induced charge separation on titanium dioxide (TiO_2) surfaces, which leads to microbial inactivation and organic mineralization without creating secondary pollution. The most important reactive oxygen species are hydroxyl radicals, which are formed by the reaction of hydroxide-ions and water molecules with the electron defects in the semiconductor (Equations (3) and (4)) (Irawaty *et al.* 2014). Superoxide anion radicals can be formed as further oxidizing agents in the electron band (Equation (5)). The electron defects themselves are also strong oxidizing agents, which can react directly with the organic compounds to be broken down (Equation (2)) (Vargas & Núñez 2010).

The degradation takes place through the reaction between C–H bonds with the reactive oxygen species under the formation of radical residuals of the hydrocarbons, which are so unstable that they disintegrate further on their own (Fox & Dulay 1993). The principal reaction between the hydroxyl radicals and the organic pollutant is shown in Equation (2). The well-known kinetics of the heterogeneous catalysis defines the step of the pollutant adsorption as the step of the kinetics which decides the velocity of the reaction. Therefore, a rough surface structure of the titanium dioxide coating will help to accelerate the disintegration of the pollutant (Didier *et al.* 2013).

Nevertheless, there are still a series of technical challenges for the application of TiO_2 catalysts to water treatment. The post-separation of the semiconductor TiO_2 catalyst after water treatment remains the major obstacle to its practicality as an industrial process (Barka *et al.* 2014). The fine particle size of the TiO_2 along with their large surface area-to-volume ratio and surface energy creates a strong tendency for catalyst agglomeration during the operation. Such agglomeration of the particles is highly detrimental given the particles' size preservation, surface-area reduction, and its reusable lifespan (Chong *et al.* 2010).

Using the catalyst designs on a fixed surface has the advantage that only a small amount of TiO_2 powder is necessary and only a small fraction ends up in the water column, thus not requiring elaborate separation. The reduction of free nanoparticles is a notable ecological benefit over the use of loose TiO_2 powder nanoparticles, which harm aquatic life forms (Adams *et al.* 2006; Haynes *et al.* 2017; Li *et al.* 2017). Photocatalytic disintegration with carrier-bound titanium dioxide catalysts provides a practical, low-cost approach for dealing with organic pollution originating from petrol-derived hydrocarbons (Cazoir *et al.* 2012), pharmaceuticals and their derivates (Schnabel *et al.* 2020), and even pathogens while possessing self-cleaning capabilities (Cabiscol 2000). The catalysts can be left on the water, utilizing a floating or fixed frame to hold them in place. Constant and predictable solar radiation is required, and no further energy use is needed. This simple low-technology method does not need trained personnel and is advantageous in acquisition and operation. These floating catalysts could be used to break down various types of pollution on the water surface with the help of solar radiation. Mineral oil-based pollution in particular that floats on the surface is a worthwhile cleaning goal for this approach.

Therefore, the goal of this study is to design and present floatable titanium dioxide-catalyst materials, which have a high surface contact with non-polar hydrocarbons that also float on the surface of the waterbody. The idea of a floatable sun driven catalyst (Qiu *et al.* 2019) was already described with bismuth-based materials (Qiu *et al.* 2019; Nasir *et al.* 2020). In this study, the goal was to investigate the suitability of three different types of floatable titanium dioxide catalysts (foam glass, glass fiber, and steel grid), provided by the Laboratories for Material Testing and Research (MFPA) Weimar, to disintegrate polar and non-polar substances in water. Ideally, these catalysts can be placed on polluted water bodies (such as water reservoirs and rain-water basins) or used as an additional cleaning stage in sewage treatment plants (Schnabel 2016; Mayer 2017),

purifying the water by removing organic pollutants like drugs and their derivates and pathogenic germs (Cabiscol 2000). In the experiments, diesel fuel served as a substitute for non-polar pollutants such as petrol-derived hydrocarbons, while the pigment methylene blue was used to investigate the degradability of polar organic substances.

EXPERIMENTAL

A series of experiments was conducted for each type of catalyst. To simulate solar radiation, an actively cooled array of UV-LEDs manufactured by Synantik (Ohrdruf, Thuringia, Germany) was used. The array has a power rating of 8 W with an efficiency of approximately 8% at 385 nm from electrical to radiometric power. Conventional 200 mL aluminum trays from the food industry with a resulting water surface area of 70 cm^2 were used as containers for each experiment. Therefore, the specific irradiation power was 91.4 W/m^2. Each aluminum tray was filled with 100 mL demineralized water, into which 100 µL (0.082 g) of diesel fuel was injected beneath the water surface. Subsequently, the fuel rose to the surface and spread evenly. The coated glass foam was put in the tray until the water surface was covered. The other photocatalytic materials (coated steel grid and glass fiber tissue) were attached to wood pieces, which helped the material float on the surface. The UV-array was placed over one of the trays at 1.5 cm on a UV light-transmissive glass panel. During the experiments, the reactors were not magnetically stirred. Various experiments with different radiation times were executed, and a new preparation for every single experiment was applied. Within the closed reactor system, there was a gas phase present, so that evaporation of volatile components occurred. To exclude the effect of evaporation, two setups were used. One was exposed to UV light, while the other was shielded from it. This allowed us to estimate the influence of evaporation and distinguish it from the effect of photocatalytic disintegration. Figures 1–3 show the floating materials.

The extraction of the remaining hydrocarbons was performed using cyclohexane. A total of 20 mL of eluent was poured into the tray, and a sample was drawn after 15 min of stirring to be analyzed via GC-FID (Agilent ChemStation 6890N and Agilent 7683B Injector). This resulted in a complete sampling of all hydrocarbons within the reactor system including adsorbed and undissolved components. The experiments using coated glass fiber and steel grit were conducted in the same manner, with the exception of the glass fibers, which were provided with a floating frame. The grits were folded such that they would remain approximately 1 mm under the water surface.

Depletion of methylene blue with natural solar radiation

Field tests were conducted in Weimar, Germany (50°N, 11°E) at 28 °C and under sunny weather on the 9 August 2017 to show the performance of the three catalysts for polar organic compounds and to include real sunlight. The experiments were performed to compare the activity of the

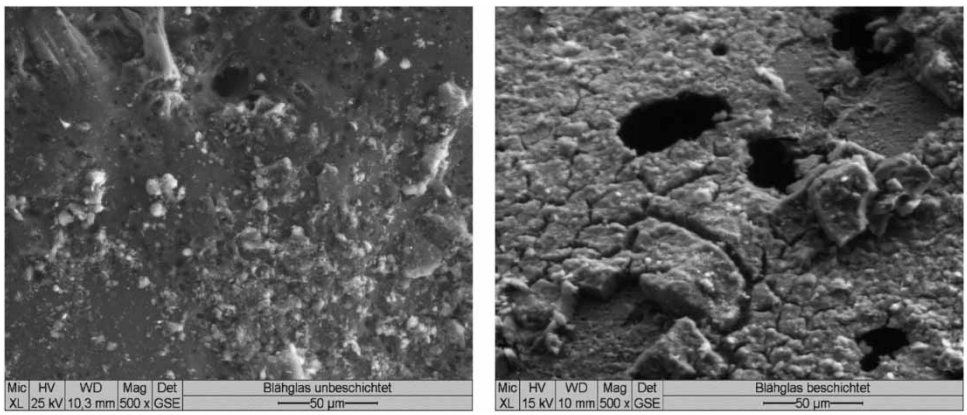

Figure 1 | Uncoated (left) and coated (right) glass foams.

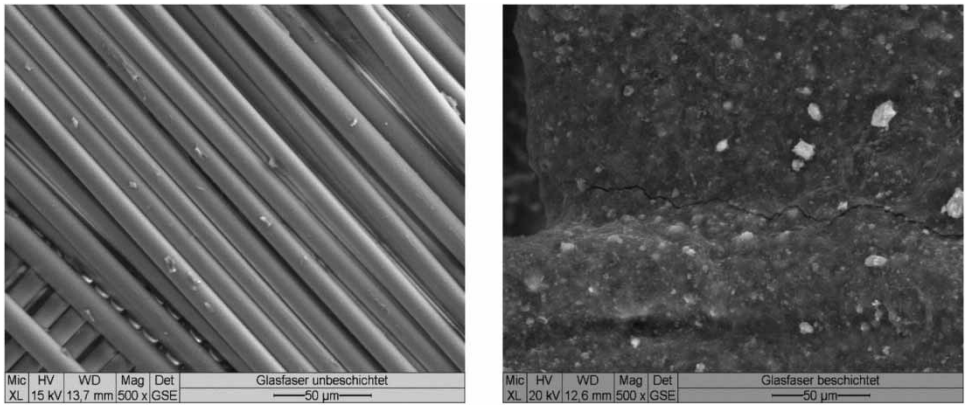

Figure 2 | Uncoated (left) and coated (right) glass fiber tissue.

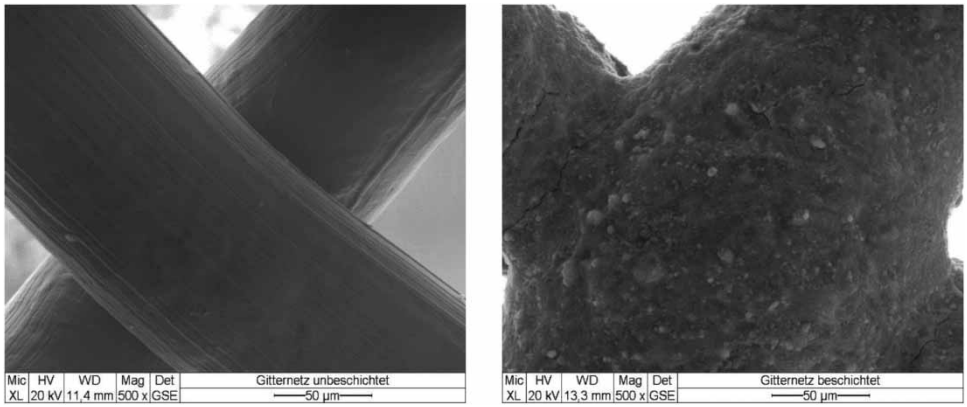

Figure 3 | Uncoated (left) and coated (right) glass steel tissue.

different materials in a homogenous solution. Methylene blue (20 µmol/L) was used as a representative of water-soluble polar substances. Discoloration and thus disintegration were quantified by a 'Merck SQ 118' photometer. The extinction was measured with a 1 cm quartz glass cuvette at a wavelength of 620 nm. The extinction has a linear relation to the methylene blue concentration, so the concentration was calculated using a 10-point calibration curve between 1 and 20 µmol/L methylene blue.

Kinetic and modeling

The photocatalytic degradation of dissolved organic substances can be described by the Langmuir–Hinshelwood equation, which is shown in the following equation (Lazar *et al.* 2012):

$$r = -\frac{dC_{eq}}{dt} = -k_{LH}\frac{K_L C_{eq}}{1 + K_L C_{eq}} \tag{6}$$

where C_{eq} is the concentration of dissolved reactant, t is the reaction time, k_{LH} is the reaction rate constant, and K_L is the adsorption coefficient of the reactant. For $K_L * \mathrm{C_{eq}} \ll 1$, Equation (6) can be simplified and the reaction rate follows a pseudo-first-order decay rate:

$$r = \frac{dC_{eq}}{dt} = -k_{LH} * \mathrm{K_L} * \mathrm{C_{eq}} = \mathrm{k} * \mathrm{C_{eq}} \tag{7}$$

This applies for small reactant concentrations or low levels of adsorption of the reactant on the catalyst surface.

For high concentrations of the reactant or strong adsorption effect, the reaction rate is no longer influenced by the reactant concentration. Equation (6) can be converted to a pseudo-zeroth-order reaction rate:

$$r = \frac{dC_{eq}}{dt} = -k_{LH} \tag{8}$$

The degradation of mixtures of mineral oil hydrocarbons, which are present as a separate phase, is further significantly influenced by the specific solubility and vapor pressures of their individual compounds. Mineral oil hydrocarbons are not miscible with water but are soluble in water to a small extent. Diesel, as a representative of the mineral oil hydrocarbons, belongs to the middle distillates, which are characterized by a boiling range of 160–390 °C and a chain length of 9–24 C atoms (Cho *et al.* 2006). The total water solubility of diesel as a mixture of mineral oil hydrocarbons is determined by the respective water solubility of the individual components. Furthermore, in the case of mineral oil mixtures, there is a mutual influence of the individual compounds, which reduces their individual solubility. With increasing chain length, a decrease of the solubility can be recognized. With the same number of C atoms, a decrease in solubility is evident in the following series: aromatics > alkenes > cycloalkanes > *i*-alkanes > *n*-alkanes. The total solubility of diesel can be classified as low and amounts to 5–20 mg/L (Speight 2020). The volatility of the individual compounds behaves analogously, whereby a decrease in volatility occurs to a greater extent with increasing molecule size compared with solubility. According to Speight (2020), the total vapor pressure of diesel mixtures is 0.05 kPa, whereby mixtures of substances above 0.01 kPa are classified as volatile.

For the photocatalytic degradation of mineral oil hydrocarbons, the degradation rate of the respective individual compound is essentially determined by its solubility. As long as the respective components are present in a separate phase, their concentration in the water phase is equal to the maximum water solubility (with the assumption of a continuous stirred-tank reactor). Due to a constant concentration, the degradation kinetics initially follows a zero-order reaction. As soon as the mineral oil phase of the respective components is no longer present due to progressive degradation, the concentration in the liquid phase is successively reduced so that the kinetics follows a first-order reaction. Parallel to this, an evaporation especially of shorter hydrocarbons takes place. As the chain length increases, the vapor pressure decreases so that the evaporation rate decreases. Meanwhile, a decrease of the solubility takes place more slowly, so that hydrocarbons of medium chain length accumulate in the water phase and are primarily decomposed photocatalytically. Longer-chain hydrocarbons continue to show a strong reduction in their solubility, so that these mineral oil components can only be decomposed very slowly by photocatalysis. For the total degradation of diesel by photocatalytic processes, the following formula was chosen to describe the reaction kinetics:

$$c_t = c_{non\ disintegrated} + c_0 * e^{k_0 * t} \tag{9}$$

In this equation, $c_{non\ disintegrated}$ is the amount of mineral oil which could not be disintegrated further during the time of the experiment. c_0 is the maximum concentration which could be disintegrated, k_0 is the exponential disintegration factor, and t is the time in hours. The kinetics show that the percentile disintegration does not depend on the concentration, but the reaction velocity depends on the concentration (Equation (9)). Within this formula, the total decrease in diesel is described by an exponential disintegration factor. As a result, both photocatalytic degradation and evaporation are represented by the disintegration factor. The influence of the evaporation was covered by an analogous data processing of the test series without the use of a catalyst. Furthermore, the photocatalytic degradation within the experiments is influenced by the mass transfer within the reactor system as well as between mineral oil and water phase, since no devices for the reactor stirring were included. For methylene blue as a water-soluble substance, the term $c_{non\ disintegrated}$ equals zero.

PHOTOCATALYTIC MATERIALS USED AND THEIR PREPARATION

Three different photocatalytic materials were used for the experiments. All three materials were coated with a layer

of titanium dioxide nanoparticles, which were sinter-fused on the hot material surface out of a waterish aerosol suspension. The load of titan dioxide was calculated so that it would be 30 g/m^2 in all experiments. The three materials used were glass foam with a diameter between 1 and 2 mm and glass fiber tissue and stainless-steel tissue with 200 µm mesh. The steel grit is made of V4A high-grade stainless steel (316 L/1.4404). An aqueous nanoparticle suspension made from anatase-modified titanium dioxide nanoparticles of 14 nm in size was used as the coating. The anatase content of the titanium dioxide was 90%, and the BET surface area of the TiO_2 particles was 50 m^2/g. The aqueous suspension was sprayed onto the heated carrier material (150–200 °C surface temperature). The fast evaporation of the solvent creates a fractal coating structure with a high inner surface (Figures 1–3). The concentration of the aqueous suspension was 10 m% titanium dioxide. The scanning electron microscope (SEM) images (Figures 1–3) show the different materials before and after the coating with the nanoparticle suspension. As can be seen in the transmission electron microscope (TEM) images, the coating of the glass tissue and the steel grit is very homogeneous while the coating of the glass foam is not as even and needs to be improved in the future to reach better photocatalytic properties. The following images show the floatability of the glass foam pearls (Figure 4(a) and 4(b)) and the other materials with the wooden floaters (Figure 4(c)).

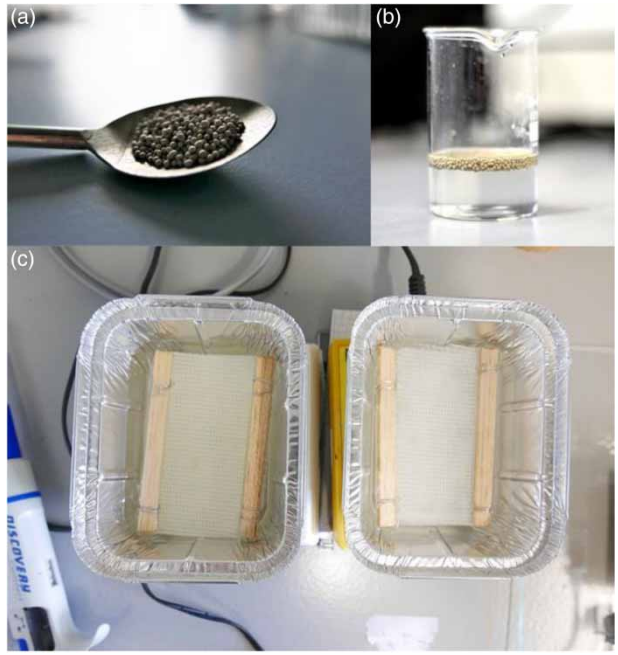

Figure 4 | (a) Glass foam, (b) floating glass foam, and (c) glass fiber with floaters.

RESULTS AND DISCUSSION

In this study, the disintegration induced by the photocatalysis of organic substances with titanium dioxide in the presence of UV light was investigated. The disintegration of UV light-exposed and non-exposed diesel fuel with different forms of catalyst was measured via gas chromatography as well as photometer measurements for methylene blue decoloring. For the evaluation of the measurements, an exponential curve fit was using the described kinetics for the disintegration of the mineral oil and methylene blue.

With the floating foam glass design, the concentration of diesel fuel could be lowered in 68 h from 688 to 271 mg/L; this equals the disintegration of 417 mg/L or 60.6%. In the experiment without UV light, the concentration decreased through evaporation of the volatile mineral oil compounds from 688 to 418 mg/L over the same time; this equals evaporation of 270 mg/L or 39%. Figure 5 shows the results as a concentration of mineral oil hydrocarbons over time. The contrast between radiated and non-radiated experiments is

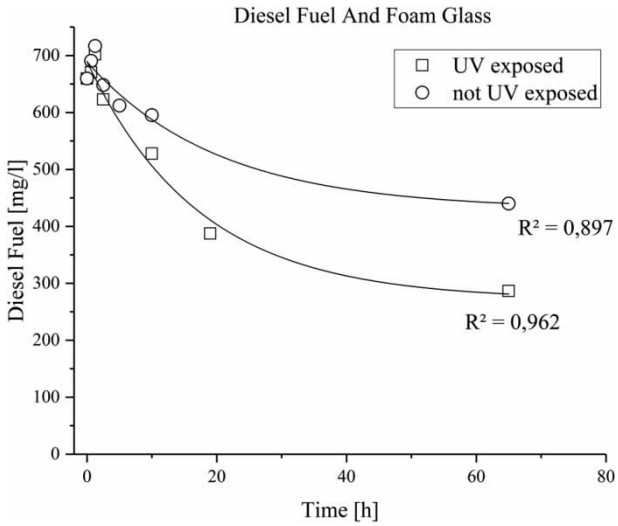

Figure 5 | Diesel fuel disintegration over time with UV light and titanium dioxide-coated foam glass. Squares represent exposure to UV; circles stand for experiments not exposed to UV. Each item represents an independent experiment. The curves were fitted with an exponential decay first order.

clearly visible throughout the tests: it is always higher in the non-radiated experiments. The calculated difference of non-radiated and radiated values in the arrangements indicates the effect of photocatalytic disintegration.

The experiments using diesel fuel were conducted with artificial UV light from LEDs because the effect of evaporation proved to be influential in an open-air setup with natural solar radiation and heating, thus corrupting the outcome. The analysis of the FID chromatograms in Figure 6 shows that the smaller compounds disintegrate faster by hydroxyl radicals than the long-chained aliphatic compounds of the mineral oil. This is due to lower volatility, solubility, and possibly lower photocatalytic reaction rates of longer-chain components. These effects overlap within the selected experimental setup, which is why this question cannot be solved completely by the existing results.

This was also shown in the fluorescent behavior of the mineral oil in the experiments after 2 h of irradiation that the mineral oil film under the photocatalytic materials was not fluorescent anymore. This provides strong evidence that especially the short aromatic compounds in the mineral oil (benzene and toluene) disintegrate faster than others. Figure 7 shows the irradiated and unirradiated samples after 2 h.

The glass fiber material has, in comparison, the highest surface area. The problem remains that this material does not float by itself and needs floaters of wood to stay close to the surface of the water. Otherwise, the contact of the catalyst and the mineral oil is not given, which may decrease reaction rate for low turbulence applications. Regardless of those problems, a higher and faster disintegration of mineral

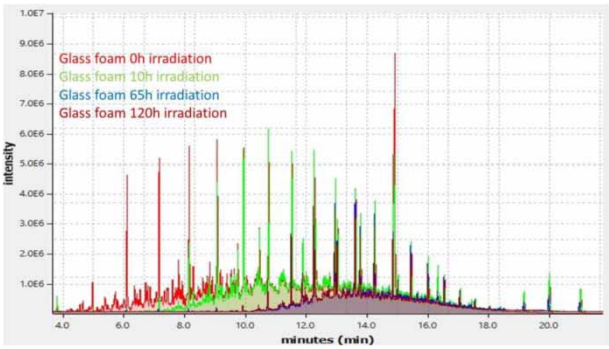

Figure 6 | Chromatogram of the analysis of hydrocarbons after different irradiation times.

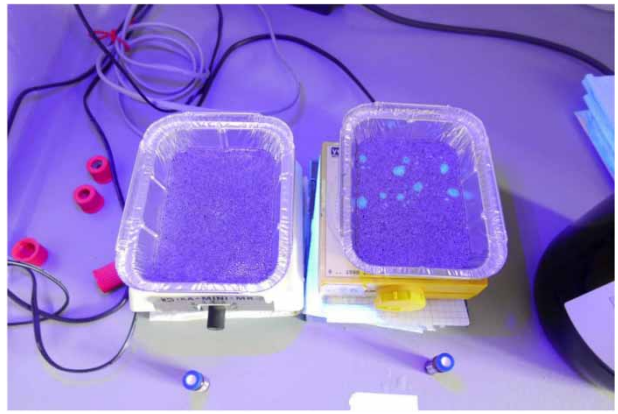

Figure 7 | Irradiated (left) and unirradiated (right) sample after 2 h using glass foam catalysts.

oil was achieved in comparison to the experiment without UV light (Figure 8). In 16 h, the evaporation was 189 mg/L (23% of the initial concentration). In the experiment with UV light, a disintegration of 591 mg/L (71% of the initial concentration) was achieved. The same effect regarding fluorescing of the mineral oil like with the glass foam could be observed. Additionally, the chromatograms were equal.

The experiment with the steel grid materials showed the smallest difference between evaporation and photocatalytic disintegration (Figure 9). The experiments showed higher variation between values, which is reflected by R^2. Presumably, insufficient adsorption of diesel fuel on the catalyst

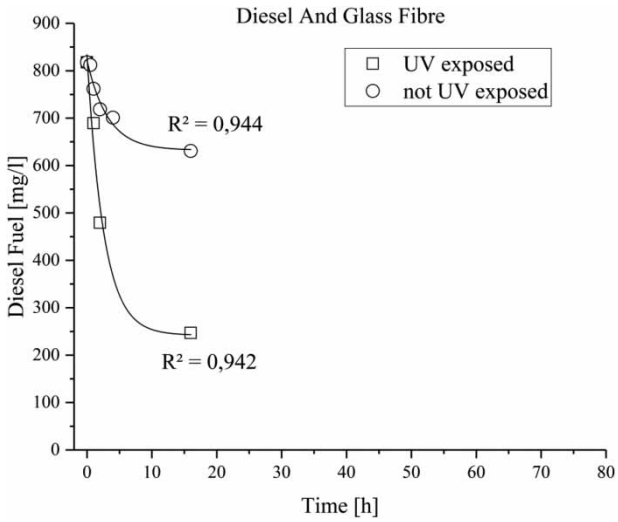

Figure 8 | Diesel fuel disintegration over time with UV light and titanium dioxide-coated glass fiber. Squares represent UV exposed; circles stand for non-UV exposed experiments. Each item represents an independent experiment. The curves were fitted with an exponential decay first order.

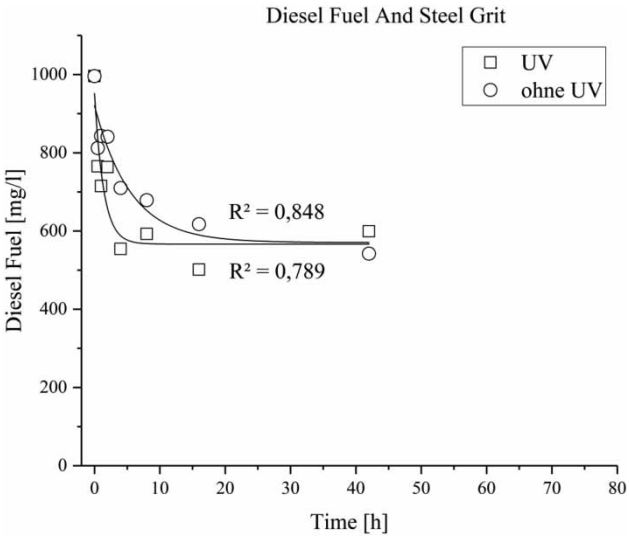

Figure 9 | Diesel fuel disintegration over time with UV light and titanium dioxide-coated steel grit. Squares represent UV exposed; circles stand for non-UV exposed experiments. Each item represents an independent experiment. The curves were fitted with an exponential decay first order.

surface led to inconsistent measurements. One hypothesis is that this effect occurs due to the greater distance of the catalyst surface from the mineral oil phase. However, glass wool, which is also a non-floatable material, showed a very high degradation rate for diesel fuel. It seems more likely that the adsorption of petroleum hydrocarbons is significantly reduced due to the electrochemical properties of steel-based catalyst carriers.

To compare all experimental setups, Table 1 provides the functions and a combination of evaporation and disintegration after 16 h. The results of the comparison showed that the difference between evaporation and photocatalytic experiment is 329 mg/L for the glass foam, 401 mg/L for the glass fiber materials, and 55 mg/L for the steel grid. This means that the glass fiber material achieved the highest photocatalytic disintegration rate, and the steel grid achieved almost no photocatalytic activity with the disintegration of mineral oil.

Thus, the decomposition of diesel fuel with coated foam glass and glass fiber proved to be promising, while the design of the coated steel grid was less efficient. Using immobilized TiO_2, a solar reactor with collectors and groundwater samples with similar hydrocarbon concentrations but a mixture of different hydrocarbons (Cho *et al.* 2006) achieved only a degradation of 10% after 4 h. When

Table 1 | Comparison of the different experiments with mineral oil

Experiment	Function	Evaporation or disintegration after 16 h
Glass foam with UV	$c_t = 271\ \text{mg/L} + 418\ \text{mg/L} * e^{(-0.057*t)}$	470 mg/L
Glass foam without UV	$c_t = 430\ \text{mg/L} + 258\ \text{mg/L} * e^{(-0.049*t)}$	141 mg/L
Glass fiber with UV	$c_t = 242\ \text{mg/L} + 591\ \text{mg/L} * e^{(-0.38*t)}$	589 mg/L
Glass fiber without UV	$c_t = 632\ \text{mg/L} + 189\ \text{mg/L} * e^{(-0.31*t)}$	188 mg/L
Steel grit with UV	$c_t = 566\ \text{mg/L} + 385\ \text{mg/L} * e^{(-0.72*t)}$	385 mg/L
Steel grit without UV	$c_t = 570\ \text{mg/L} + 349\ \text{mg/L} * e^{(-0.18*t)}$	330 mg/L

switching to 0.2% TiO_2 slurry 80% of the hydrocarbons could be degraded after 4 h. In these experiments, the measured solar irradiation power per surface was 16 W/m^2, which is lower than the value chosen in this paper. However, due to the use the reactor designs, a higher specific irradiation surface of 0.55 m^2/L was created. The volume-specific irradiation power of 8.8 W/L is of a similar order of magnitude to the selected experimental design (6.37 W/L). The higher degradation rate of the hydrocarbons (Cho *et al.* 2006) can be explained by the use of groundwater samples which only contain the soluble contents of mineral oil hydrocarbons. In conclusion, it is shown that the floating, carrier-bound catalysts can achieve nearly the same reaction velocity for the degradation of mineral oil as particulate material.

The experiments with methylene blue depletion were conducted with real sunlight in sunny weather conditions, as direct solar radiation had – in contrast to the experiments with diesel fuel – no observable effect on dye concentration via evaporation. As shown in Figure 10, glass foam and steel grit catalysts could disintegrate the pigment more efficiently and in a shorter time than the glass foam. The control of uncoated glass foam had no observable effect on the dye. The attainable degradation was much higher than in the experiments with diesel fuel.

Decoloring of methylene blue solution for steel grit yielded up to 99.1% decoloring after 4 h, for glass fiber 96.6% after 6 h, and for glass foam 56.4% after 6 h. The

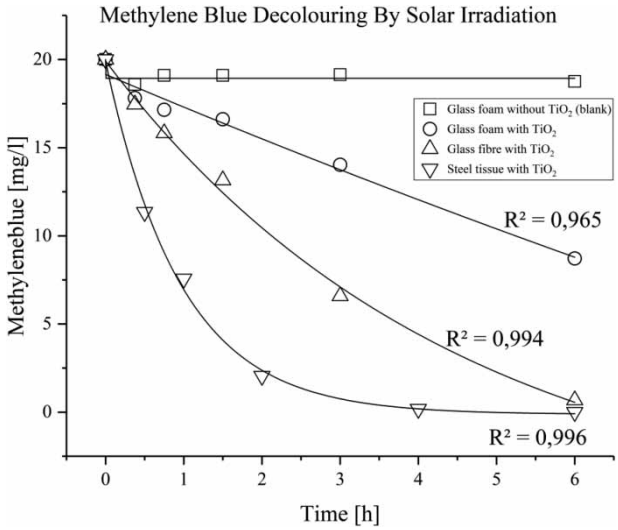

Figure 10 | Methylene blue disintegration over time with natural sunlight and foam glass coated with titanium dioxide, glass fiber, and steel grit as well as uncoated foam glass. Each item represents an independent experiment.

trend line fits well with the values measured with exponential decay of the first order (except foam glass without TiO_2), which diverges from it only to a small extent as shown by its correlation (R^2). The catalysts investigated showed a higher effect on the polar substance methylene blue than on the diesel fuel. Foam glass could disintegrate over 50% of methylene blue after 6 h, while only foam glass was able to mineralize 47% of diesel fuel concentration after 16 h. Glass fiber and steel grit could diminish methylene blue concentration by 96.6% after 4 h 99.1% after 6 h, respectively. Given that the experiments with diesel and glass fiber/steel grit produced inconsistent results, the outcome of the methylene blue examinations, in contrast, showed that the capability of the catalysts relies mostly on adequate adsorption and contact of the organic compounds to make them available for photocatalysis. The non-polar nature of hydrocarbons and the polarity of dissolved methylene blue may also play an important role during adsorption. Table 2 provides the exponential functions of the methylene blue experiment as well as the half-life time for the different materials.

Table 2 | Comparison of the methylene blue discoloration with sunlight

Experiment	Function	Half-life time
Glass foam	$c_t = -1.72$ (µmol/L)/h*t	5.8 h
Glass fiber	$c_t = c_0\ e^{(-0.22*t)}$	2.4 h
Steel grit	$c_t = c_0\ e^{(-1.03*t)}$	0.6 h

CONCLUSION

Within the scope of this work, it could be demonstrated that carrier-bound TiO_2 catalysts can achieve similar degradation rates in their application as floating catalysts to those achieved by particulate catalyst material. However, the investigated catalysts show a slightly reduced reaction rate, which in practical applications should be compensated by a much easier handling. The treatment of mineral oil phases in larger water bodies represents a promising application of this technology. In the carried out experiments, the floating design of foam glass coated with titanium dioxide could reduce the concentration of diesel fuel by 329 mg/L in 16 h; the submerged designs for coated glass fiber and coated steel grit could reduce methylene blue concentration by 96.6% after 4 h and 99.1% after 6 h, respectively. In relation to an application for mineral oil degradation, the question arises as to how the behavior of dissolved mineral oil hydrocarbons in large water bodies with high dilution potentials and higher turbulence is influenced by the positioning of the catalysts. It is assumed that the distance between catalyst and mineral oil phase has a significant influence on the degradation rate. Given this context, the use of self-floatable catalysts, such as glass foam as a carrier material, seems to be promising. The conducted experiments have shown that this material is generally suitable but shows a lower activity. An optimization of the coating process is, therefore, recommended.

For the degradation of diesel fuel, the experiments further showed a limitation to the maximum amount accessible to photocatalytic degradation. Photocatalytic degradation requires a dissolved state for the compounds to be oxidized. For longer-chain mineral oil components, this is only given to a very limited extent. It should be noted that highly insoluble and correspondingly less mobile substances usually have an equally low ecotoxicological impact potential. It would also be feasible to counteract this effect by using solubilizers (e.g. surfactants). In addition, a loss of function is to be feared in the permanent reactor operation due to the retention of a highly viscous, almost inert mineral oil phase. With regard to the development of an effective technical application, the

investigation of permanent modes of operation represents an essential step and should possibly be taken into account within future research projects.

A comparison of the tests with mineral oil and methylene blue revealed significant differences in the activity of the catalysts investigated. The catalysts with steel grids as carrier material showed almost no activity for diesel fuel, while they degraded methylene blue at a very high rate. The catalysts with glass foam and glass fiber as carrier material showed the same ranking in activity for both groups of substances. In addition to varying solubility, the investigated substance groups differed substantially with respect to their molecular charge. Catalysts fixed on conductive stainless steel appear to show an affinity for the degradation of polar substances. An increased positive potential on the catalyst would cause an increased adsorption of polar substances and thus explain their higher reaction rate according to the Langmuir–Hinshelwood kinetic. Furthermore, by discharging excited electrons to a counter electrode, the recombination rate of the electron-hole sites is reduced, which can increase the quantum efficiency of the catalyst. Increased degradation rates of photoelectric catalysis using an external voltage source are described in Song *et al.* (2019); Collivignarelli *et al.* (2020); Wang *et al.* (2020). It is also known that electrical potentials are generated by excitation of the semiconductor material titanium dioxide (Sclafani & Herrmann 1996; Li & Shen 2006; Suhadolnik *et al.* 2016). The influence of the carrier material on this electrochemical system has not yet been sufficiently investigated for carrier-based photocatalytic applications. Within this work, overlapping effects of solubility and electric charge were found, which is why an exact quantification of each process is not possible. Therefore, there is a need for further research on the influence of the carrier materials on the obtainable reaction rates for different groups of substances.

Apart from the main objective of the study, it can be stated that carrier-bound solar photocatalysis offers an energy-neutral and low-maintenance option for the oxidation of dissolved substances. While in most applications it is not possible to achieve a continuously operating treatment stage due to varying solar radiation, this technology could provide a supporting purification stage which, in the case of solar irradiation, allows energy and more cost-intensive conventional processes to be relieved. For these applications, the floatability of the catalysts only influences the absorption of solar radiation by the water layer above the catalyst. Due to the higher activity, the use of glass wool or steel grit catalysts, equipped with floating frames or fixed installations, seems to be reasonable. An application idea would be to use the free surfaces of existing post clarification plants for solar photocatalysis as a supplementary measure for the elimination of micro pollutants. The use of carrier-bound catalysts as a sole purification stage for micro pollutants or other organic compounds is also possible. In this case, an artificial irradiation source is required to achieve a permanent and efficient system operation. UV-LEDs have proven to be an efficient source of UV light and electricity consumption.

DATA AVAILABILITY STATEMENT

All relevant data are included in the paper or its Supplementary Information.

REFERENCES

Adams, L. K., Lyon, D. Y. & Alvarez, P. J. J. 2006 Comparative eco-toxicity of nanoscale TiO_2, SiO_2, and ZnO water suspensions. *Water Research* **40** (19), 3527–3532. https://doi.org/10.1016/j.watres.2006.08.004.

Barka, N., Abdennouri, M., Boussaoud, A., Galadi, A., Baâlala, M., Bensitel, M., Sahibed-Dine, A., Nohair, K. & Sadiq, M. 2014 Full factorial experimental design applied to oxalic acid photocatalytic degradation in TiO_2 aqueous suspension. *Arabian Journal of Chemistry* **7** (5), 752–757. https://doi.org/10.1016/j.arabjc.2010.12.015.

Bergmann, A., Fohrmann, R. & Weber, F. A. 2011 *Zusammenstellung von Monitoringdaten zu Umweltkonzentrationen von Arzneimitteln (Compilation of Monitoring Data on Environmental Concentrations of Pharmaceuticals)*. Text 66/2012, Umweltbundesamt, Dessau-Roßlau.

Cabiscol, E. 2000 Oxidative stress in bacteria protein damage by reactive oxygen species. *International Microbiology* **3** (1), 3–8.

Cazoir, D., Fine, L., Ferronato, C. & Chovelon, J.-M. 2012 Hydrocarbon removal from bilgewater by a combination of air-stripping and photocatalysis. *Journal of Hazardous Materials* **235–236**, 159–168. https://doi.org/10.1016/j.jhazmat.2012.07.037.

Cho, I.-H., Kim, L.-H., Zoh, K.-D., Park, J.-H. & Kim, H.-Y. 2006 Solar photocatalytic degradation of groundwater contaminated with petroleum hydrocarbons. *Environmental Progress* **25** (2), 99–109. https://doi.org/10.1002/ep.10124.

Chong, M. N., Jin, B., Chow, C. W. K. & Saint, C. 2010 Recent developments in photocatalytic water treatment technology: a review. *Water Research* **44** (10), 2997–3027. https://doi.org/10.1016/j.watres.2010.02.039.

Collivignarelli, M. C., Abbà, A., Carnevale Miino, M., Arab, H., Bestetti, M. & Franz, S. 2020 Decolorization and biodegradability of a real pharmaceutical wastewater treated by H_2O_2-assisted photoelectrocatalysis on TiO_2 meshes. *Journal of Hazardous Materials* **387**, 121668.

Didier, R., Valerie, K. & Nicolas, K. 2013 Immobilization of a semiconductor photocatalyst on solid supports: methods, material, and application. In: *Photocatalysis and Water Purification, Chapter 6* (P. Pichat & M. Lu, eds). Wiley-VCH Verlag GmbH Co.KGaA, Weinheim, pp. 145–178.

Fox, M. A. & Dulay, M. T. 1993 Heterogeneous photocatalysis. *Chemical Reviews* **93**, 341–357.

Haynes, V. N., Evan Ward, J., Russell, B. J. & Agrios, A. G. 2017 Photocatalytic effects of titanium dioxide nanoparticles on aquatic organisms – current knowledge and suggestions for future research. *Aquatic Toxicology* **185**, 138–148. https://doi.org/10.1016/j.aquatox.2017.02.012.

Irawaty, W., Soetaredjo, F. E. & Ayucitra, A. 2014 Understanding the relationship between organic structure and mineralization rate of TiO_2-mediated photocatalysis. *Procedia Chemistry* **9**, 131–138. https://doi.org/10.1016/j.proche.2014.05.016.

Lazar, M., Varghese, S. & Nair, S. 2012 Photocatalytic water treatment by titanium dioxide: recent updates. *Catalyst* 572–601. https://doi.org/10.3390/catal2040572.

Li, M. C. & Shen, J. N. 2006 Photoelectrochemical oxidation behavior of organic substances on TiO_2 thin-film electrodes. *Journal of Solid State Electrochemistry* **10** (12), 980–986. https://doi.org/10.1007/s10008-005-0043-5.

Li, Z., Wang, X., Ma, B., Wang, S., Zheng, D., She, Z. & Guo, L. 2017 Long-term impacts of titanium dioxide nanoparticles (TiO_2 NPs) on performance and microbial community of activated sludge. *Bioresource Technology* **238**, 361–368. https://doi.org/10.1016/j.biortech.2017.04.069.

Mayer, M. 2017 *Photokatalytische Ozonierung zur Spurenstoffelimination aus Kommunalem Abwasser (Reduction of Trace Pollutants in Waste Water by Photocatalytic Ozonation)*. Master's Thesis, Bauhaus-Universität Weimar, Weimar.

Mehrjouei, M., Müller, S. & Möller, D. 2015 A review on photocatalytic ozonation used for the treatment of water and wastewater. *Chemical Engineering Journal* **263**, 209–219.

Nasir, A. M., Jaafar, J., Aziz, F., Yusof, N., Salleh, W. N. W., Ismail, A. F. & Aziz, M. 2020 A review on floating nanocomposite photocatalyst: fabrication and applications for wastewater treatment. *Journal of Water Process Engineering* **36**, 101300. https://doi.org/10.1016/j.jwpe.2020.101300.

Nosaka, Y. & Nosaka, A. Y. 2013 Identification and roles of the active species generated on various photocatalysts. In: *Photocatalysis and Water Purification, Chapter 1* (P. Pichat & M. Lu, eds). Wiley-VCH Verlag GmbH Co.KGaA, Weinheim, pp. 3–24.

Pedanekar, R. S., Shaikh, S. K. & Rajpure, K. Y. 2020 Thin film photocatalysis for environmental remediation: a status review. *Current Applied Physics* **20** (8), 931–952. https://doi.org/10.1016/j.cap.2020.04.006.

Pinnekamp, J., Keysers, C., Montag, K. & Veltmann, D. 2010 *Elimination von Mikroschadstoffen – Stand der Wissenschaft (Elimination of Micropollutants – State of the Art)*. Gewässerschutz-Wasser-Abwasser.

Pitre, S. P., Yoon, T. & Scaiano, T. 2017 Titanium dioxide visible light photocatalysis: surface association enables photocatalysis with visible light irradiation. *Chemical Communications* **31** (53), 4335–4338.

Qiu, H., Hu, J., Zhang, R., Gong, W., Yu, Y. & Gao, H. 2019 The photocatalytic degradation of diesel by solar light-driven floating BiOI/EP composites. *Colloids and Surfaces A: Physicochemical and Engineering Aspects* **583**, 123996. https://doi.org/10.1016/j.colsurfa.2019.123996.

Schnabel, T. 2016 *Photokatalytischer Abbau von Medikamentenrückständen als Möglichkeit für eine 4.Reinigungsstufe in kommunalen Kläranlagen (Photocatalytic Breakdown of Drug Residues as a Possibility for a 4th Purification Stage in Municipal Sewage Treatment Plants)*. Master theses, Bauhaus-Universität Weimar.

Schnabel, T., Mehling, S. & Londong, J. 2020 Hydrogen-peroxide-assisted photocatalytic water treatment for the removal of anthropogenic trace substances from the effluent of wastewater treatment plants. *Water Science and Technology* **82** (10), 2019–2028. https://doi.org/10.2166/wst.2020.481.

Sclafani, A. & Herrmann, J. M. 1996 Comparison of the photoelectronic and photocatalytic activities of various anatase and rutile forms of titania in pure liquid organic phases and in aqueous solutions. *The Journal of Physical Chemistry* **100** (32), 13655–13661.

Song, T., Li, R., Li, N. & Gao, Y. 2019 Research progress on the application of nanometer TiO_2 photoelectrocatalysis technology in wastewater treatment. *Science of Advanced Materials* **11** (2), 158–165. https://doi.org/10.1166/sam.2019.3411.

Speight, J. G. 2020 *Handbook of Industrial Hydrocarbon Processes*, 2nd edn. Gulf Professional Publishing, an imprint of Elsevier, Cambridge, MA.

Suhadolnik, L., Pohar, A., Likozar, B. & Čeh, M. 2016 Mechanism and kinetics of phenol photocatalytic, electrocatalytic and photoelectrocatalytic degradation in a TiO_2-nanotube fixed-bed microreactor. *Chemical Engineering Journal* **303**, 292–301.

Vargas, R. & Núñez, O. 2010 Photocatalytic degradation of oil industry hydrocarbons models at laboratory and at pilot-plant scale. *Solar Energy* **84** (2), 345–351. https://doi.org/10.1016/j.solener.2009.12.005.

Wang, Y., Zu, M., Zhou, X., Lin, H., Peng, F. & Zhang, S. 2020 Designing efficient TiO_2-based photoelectrocatalysis systems for chemical engineering and sensing. *Chemical Engineering Journal* **381**, 122605.

Weichgrebe, D., Geißen, S. U. & Vogelpohl, A. 1991 *Deponiesickerwasserbehandlung in Biologischen Systemen (Landfill Leachate Treatment in Biological Systems)*. Tagungsband der GVC-Jahrestagung, (Kurzfassung der Vorträge und Poster), Aachen.

First received 30 November 2020; accepted in revised form 20 March 2021. Available online 30 March 2021